Al-Qadisiyah Journal of Pure Science

ISSN(Printed): 1997-2490 ISSN(Online): 2411-3514

DOI: 10.29350/jops

Al-Qadisiyah Journal of Pure Science

Heavy Metals in Ambient Air and Deposited Dust Across Land-Use Types in Najaf, Iraq: Spatial Patterns, Health-Risk Readiness, and the Role of Dust Storms and Pilgrimage Traffic

Zahraa A. Al-Hamza[1], Lujain Ebrihem Hussien[2]

Received: 04/05/2026; Revised: 13/05/2026; Accepted: 17/05/2026.

Abstract

Background: Urban deposited dust and ambient particulate matter are important reservoirs of potentially toxic metals in arid cities where traffic, workshops, construction, and dust storms coexist. Najaf, Iraq, also experiences periodic traffic and pedestrian-pressure increases related to religious visitation.

Purpose: This study analysed Pb, Cd, and Ni in a station-month dataset from six land-use stations in Najaf between October and March, focusing on spatial gradients, monthly variation, metal co-variation, and readiness for defensible health-risk assessment.

Methods: Settled dust samples were collected monthly from six land-use stations, yielding 36 station-month observations for each metal. After wet-acid digestion, metals were determined by atomic absorption spectrometry, with graphite furnace AAS used for low-level toxic metals. Station and monthly means, fold enrichment relative to the semi-rural reference site, Pearson correlations, one-way ANOVA, Kruskal–Wallis tests, and a normalized hotspot-priority score were calculated.

Findings: S5 showed the highest mean Pb, Cd, and Ni concentrations, whereas S6 showed the lowest. Compared with S6, S5 was 2.30-, 3.93-, and 2.76-fold higher for Pb, Cd, and Ni, respectively. Station-level differences were significant for all metals, while monthly differences were weaker and non-significant. Metals were strongly correlated.

Conclusion: Metal distribution was controlled mainly by land use rather than month. Industrial-transport and pilgrimage/traffic-influenced zones require priority monitoring, while definitive HQ, HI, and ILCR modelling needs complete exposure-pathway and toxicity-parameter specification.

Keywords: atmospheric dust; pilgrimage traffic; dust storms; health-risk assessment; land use.

1. Introduction

Deposited atmospheric dust and road dust are important reservoirs and transport media for potentially toxic metals in urban environments. Pb, Cd, and Ni are of particular concern because they can persist in surface dust, accumulate near anthropogenic activities, and be re-suspended during dry weather, vehicle movement, construction work, and dust-storm events [1-5]. Although heavy-metal contamination in urban dust has been studied in several Iraqi and regional settings, there is still limited published evidence linking Pb, Cd, and Ni distributions with operational land-use categories specifically within Najaf. This local evidence gap justifies a land-use-based analysis rather than a general city-level description.

Najaf presents a distinctive context for assessing dust-bound metal contamination. It is an arid urban system where ordinary road traffic, industrial-transport fringes, commercial activity, and intermittent visitation peaks coexist. Pilgrimage-related mobility may increase vehicle idling, road-dust re-suspension, temporary commercial activity, and pedestrian exposure in narrow urban corridors. In the broader Iraqi and Middle Eastern context, recent work has also emphasized the role of dust storms and synoptic transport in increasing particulate-matter levels and mobilizing mineral or contaminated dust [11-15].

The distinction between ambient-air concentration and settled/deposited-dust concentration was handled explicitly because the supplied study context refers to ambient air/deposited dust but reports metals in ppm. In dust and soil-like matrices, ppm is generally interpreted as mg/kg solid material, whereas ambient-air exposure assessment requires volumetric units such as micrograms/m3 or a documented conversion from filter mass and sampled air volume. Therefore, the present manuscript treats the data as settled-dust concentrations and does not convert them into volumetric air concentrations [6-10].

The objectives of this manuscript were threefold. First, the reported Pb, Cd, and Ni results were converted into a reproducible station-month analysis. Second, spatial and monthly trends were evaluated across six operational land-use settings. Third, the manuscript determined the level of health-risk assessment that can be scientifically supported by the current dataset and identified the minimum additional metadata needed for defensible HQ, HI, and ILCR calculations.

2. Materials and Methods

2.1 Study design and land-use stations.

The study was designed as a land-use-based environmental monitoring analysis across six stations in Najaf, Iraq, measured monthly from October to March. This produced 36 station-month observations for each metal (Pb, Cd, and Ni). Table 1 summarizes the operational land-use classifications used in the analysis. Verified GIS coordinates were not available in the supplied experimental file; therefore, the sampling-design figure is presented as a schematic rather than a georeferenced map.

Table 1. Land-use classification of the six monitoring stations.

Station	Land-use type	Operational description
S1	Mixed residential–commercial	Urban mixed-use area with moderate traffic and commercial activity.
S2	High-traffic arterial corridor	Major road corridor with heavy mixed vehicle movement.
S3	Pilgrimage/religious district	High visitation area influenced by shrine access, congestion, and pedestrian/vehicle flux.
S4	Low-density residential suburb	Peripheral residential area with lower local traffic intensity.
S5	Industrial–transport periphery	Workshops, fuel/transport activity, freight movement, or industrial edge effects.
S6	Semi-rural reference site	Lower-intensity semi-rural reference away from major point sources.

2.2 Sampling matrix, collection, and laboratory analysis.

Settled dust was used as the environmental matrix for trace-metal determination. Samples were obtained from six land-use stations in Najaf, Iraq, during the October-March monitoring period. Because the results are reported in ppm for a solid dust matrix, concentrations are interpreted as mg/kg dust-equivalent unless the original laboratory worksheet specifies a different reporting basis. The manuscript therefore does not treat the values as direct volumetric ambient-air concentrations.

Trace metals in settled dust samples were determined using atomic absorption spectrometry. A flame AAS (AA-7000, Shimadzu, Japan) was used for elements present at higher levels, whereas graphite furnace AAS (240Z AA, Agilent Technologies, USA) was used for low-level toxic metals, including Pb, Cd, Ni, and Cr. Sample preparation was performed by wet-acid digestion with concentrated nitric acid (HNO3) and hydrogen peroxide (H2O2), followed by dilution with deionized water to a known final volume before instrumental analysis.

Quality assurance and quality control (QA/QC) included reagent blanks, calibration blanks, calibration verification standards in each analytical batch, spike-recovery tests, and laboratory control samples. Spike recoveries within 90-110% were considered acceptable, and all batches met predefined acceptance criteria for calibration linearity, recovery, and blank levels. Method detection limits (LOD) and limits of quantification (LOQ) were calculated as three and ten times the standard deviation of the reagent blank signal, respectively. These limits typically fell in the low micrograms/L range in solution, corresponding to low micrograms/g levels in the dust matrix after digestion and dilution correction.

2.3 Unit basis and health-risk assessment readiness

The available files require interpretation of HQ, HI, and ILCR, but these indices need an explicit exposure pathway, compatible concentration unit, exposure frequency and duration, body weight, ingestion/inhalation rates, toxicity reference values, and, for inhalation assessment, either a direct air concentration or a validated conversion based on sampled air volume or dust loading. Although the analytical method and QA/QC framework are now described, the files still do not provide complete exposure-pathway metadata, particle-size fraction, air-volume conversion, population exposure assumptions, or toxicity-value selection. Therefore, final numerical HQ, HI, and ILCR values are not calculated in this manuscript. Instead, a relative hotspot score is used to rank stations for follow-up exposure assessment [3,7-10].

2.4 Statistical analysis

Statistical analysis was performed at the station-month level. Descriptive statistics were calculated for each station and month. The 36 paired station-month observations of Pb, Cd, and Ni were used to calculate Pearson correlation coefficients. Exploratory group comparisons used one-way ANOVA and Kruskal-Wallis tests to compare stations and months because the source file provided one summarized value per station-month cell and did not include replicate-level laboratory measurements. Statistical significance was set at $p < 0.05$. The LSD values shown in the supplied results were retained as reported study outputs and were not recalculated because raw replicate-level data were unavailable. The use of Kruskal-Wallis testing as a non-parametric method for comparing three or more groups followed standard statistical guidance [16].

3. Results

3.1 Spatial distribution among the land-use types.

All three metals showed a consistent and statistically significant spatial gradient. Station-level comparisons were significant for Pb, Cd, and Ni by both ANOVA and Kruskal-Wallis tests ($p < 0.001$; Table 4), confirming that differences between land-use stations were significant at $p < 0.05$. The common station ranking for all three metals was S5 > S3 > S2 > S1 > S4 > S6. S5, the industrial-transport periphery, recorded the highest station mean for all metals, whereas S6, the semi-rural reference site, recorded the lowest mean. Based on the station means and reported LSD outputs, the largest separations were between S5 and S6, S5 and S4, and S3 and S6. These findings support a land-use-related anthropogenic source gradient.

Table 2. Station-level descriptive statistics and normalized hotspot score.

Station	**Land-use**	**Pb ppm, mean ± SD**	**Cd ppm, mean ± SD**	**Ni ppm, mean ± SD**	**Hotspot score**
S1	Mixed residential–commercial	35.77 ± 4.17	1.062 ± 0.177	31.82 ± 4.32	32.1
S2	High-traffic arterial corridor	41.44 ± 4.64	1.306 ± 0.248	38.40 ± 5.06	49.0
S3	Pilgrimage/religious district	49.95 ± 5.22	1.791 ± 0.294	46.72 ± 5.39	75.2
S4	Low-density residential suburb	30.51 ± 3.91	0.808 ± 0.165	26.10 ± 3.63	16.2
S5	Industrial–transport periphery	57.23 ± 4.44	2.272 ± 0.293	54.89 ± 4.87	100.0
S6	Semi-rural reference site	24.91 ± 3.27	0.578 ± 0.127	19.91 ± 2.86	0.0

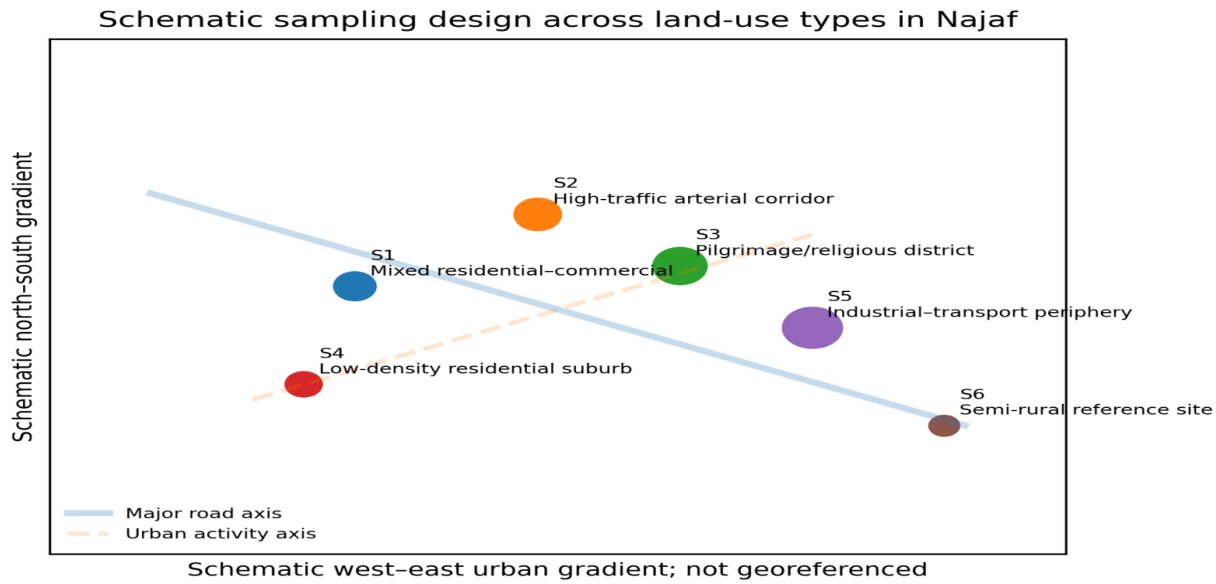

Figure 1. Schematic sampling design across land-use types in Najaf. Bubble size represents the relative hotspot score. The figure is not georeferenced because verified coordinates were not available in the uploaded files.

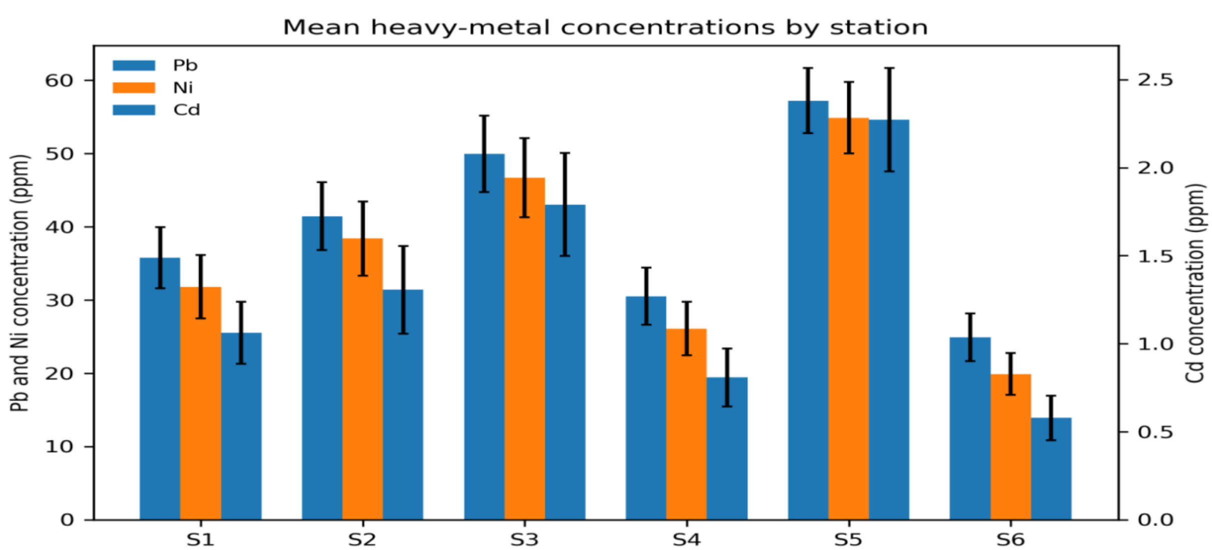

Figure 2. Mean Pb, Cd, and Ni concentrations by station. Error bars represent standard deviation across monthly observations.

3.2 Monthly variation

Monthly means were highest in October and lowest in January for all three metals. The pattern is compatible with stronger early-season dust re-suspension and lower winter dust activity. However, month-level ANOVA was not statistically significant for Pb ($p = 0.597$), Cd ($p = 0.632$), or Ni ($p = 0.657$), indicating that temporal variation was weaker than spatial land-use variation. Because the supplied files did not include confirmed dust-storm dates, wind speed, precipitation, or traffic-count data, dust storms and pilgrimage traffic are interpreted as plausible contributors rather than proven causal drivers.

Table 3. Monthly mean concentrations and LSD values reported in the uploaded results.

Month/statistic	Pb ppm	Cd ppm	Ni ppm
Oct	44.81	1.551	41.21
Nov	43.17	1.430	39.47
Dec	36.37	1.125	33.10
Jan	33.94	0.983	29.94
Feb	38.88	1.277	35.06
Mar	42.64	1.450	39.06
LSD: station	0.265	0.0177	0.243
LSD: month	0.265	0.0177	0.243
LSD: station × month	0.649	0.0434	0.596

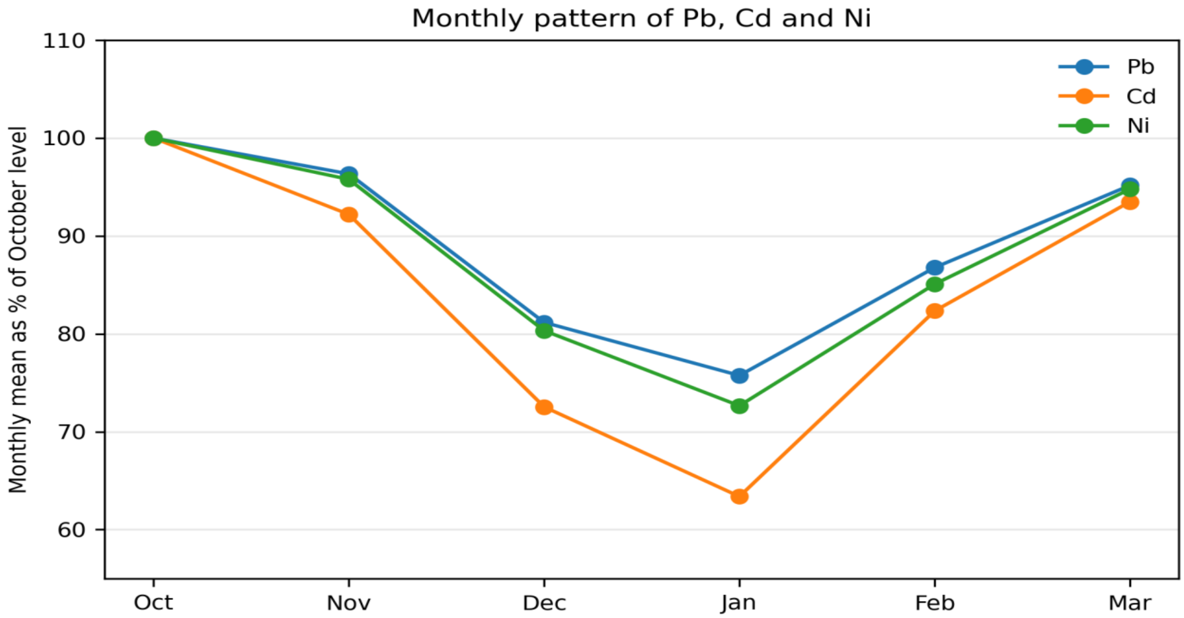

Figure 3. Monthly pattern expressed as percentage of October mean concentration. The index allows Pb, Cd, and Ni to be compared on one scale.

3.3 Statistical comparison and metal co-variation

The statistical analysis supported the dominance of the spatial signal. Station-level ANOVA p-values were < 0.001 for Pb, Cd, and Ni, and station eta-squared values were high (0.886-0.896). Kruskal-Wallis tests were also significant for all three metals ($p < 0.001$). By contrast, month-level comparisons were not significant in the same exploratory framework. The metals were almost perfectly correlated across the 36 station-month observations: Pb-Cd $r = 0.994$, Pb-Ni $r = 0.999$, and Cd-Ni $r = 0.994$, with all p-values < 0.001. This pattern supports a shared source mixture, co-deposition in the same dust mass, or a common land-use intensity factor controlling all three metals simultaneously.

Table 4. Exploratory station and month comparison statistics calculated from the reconstructed station-month matrix.

Metal	Station F	Station p	Station eta²	Station H	KW p	Month F	Month p	Month eta²
Pb	47.25	<.001	0.887	31.14	<.001	0.74	0.597	0.110
Cd	46.77	<.001	0.886	31.02	<.001	0.69	0.632	0.104
Ni	51.76	<.001	0.896	31.62	<.001	0.66	0.657	0.099

Table 5. Pearson correlation matrix for Pb, Cd, and Ni across 36 station-month observations.

Variable	Pb	Cd	Ni
Pb	1.000	0.994	0.999
Cd	0.994	1.000	0.994
Ni	0.999	0.994	1.000

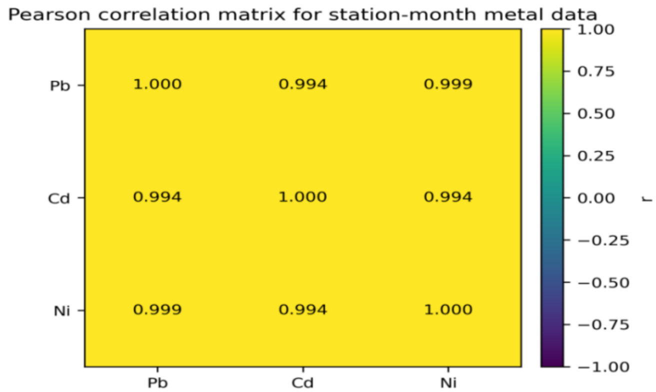

Figure 4. Pearson correlation heatmap for Pb, Cd, and Ni. All off-diagonal correlations were significant at $p < .001$.

3.4 Health-risk interpretation and hotspot prioritization

The normalized hotspot score ranks stations by the combined relative magnitude of Pb, Cd, and Ni. It is not a substitute for HQ, HI, or ILCR. S5 reached the maximum score (100), followed by S3 (75.2), S2 (49.0), S1 (32.1), S4 (16.2), and S6 (0). Thus,

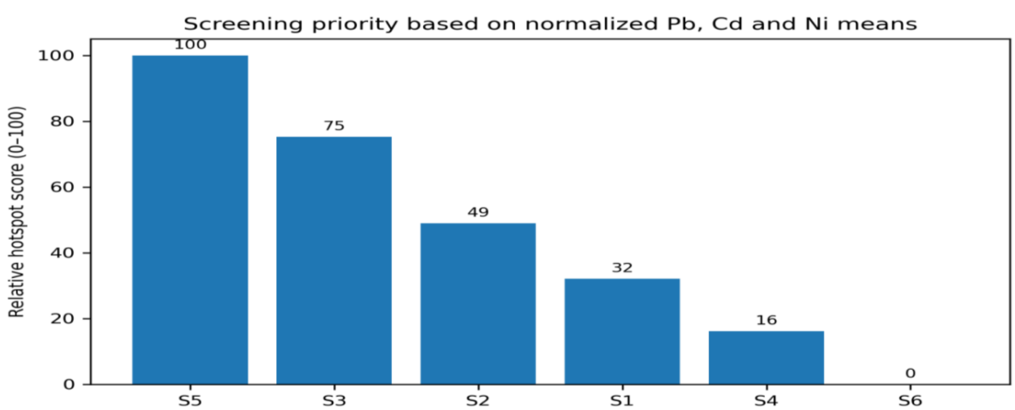

S5 and S3 should be prioritized for confirmatory sampling, exposure-pathway characterization, and population-specific risk assessment.

Figure 5. Relative hotspot score based on normalized station means for Pb, Cd, and Ni. This screening score ranks sampling priorities; it is not an HQ, HI, or ILCR estimate.

Table 6. Health-risk assessment readiness and evidence gaps.

Component	Current status	Requirement for Q1-level risk reporting
Concentration basis	Settled dust reported in ppm; interpreted as mg/kg dust-equivalent	Report the final laboratory basis explicitly and avoid treating ppm dust as micrograms/m3 air
Inhalation HQ/HI	Not defensible from ppm dust values alone	Requires air concentration or validated air-volume/dust-loading conversion
Ingestion HQ/HI	Potentially feasible for settled dust if exposure assumptions are provided	Requires ingestion rate, exposure frequency, body weight, exposure duration, RfD values, and age group
Dermal risk	Not calculated	Requires adherence factor, skin area, absorption factor, and dust matrix confirmation
ILCR	Not calculated	Requires verified carcinogenic slope factors or inhalation unit risks and exposure unit compatibility
Priority stations	S5 then S3	Based on normalized contamination score only
Analytical QA/QC	AAS method described; blanks, calibration verification, laboratory control samples, and spike recovery 90-110% reported as acceptable	Provide metal-specific LOD/LOQ and batch QC values in the final manuscript or supplementary file

4. Discussion

The main interpretation of the dataset is that land-use, rather than sampling month, controlled the distribution of Pb, Cd, and Ni. The highest station was S5, the industrial-transport periphery, with Pb = 57.23 +/- 4.44 ppm, Cd = 2.272 +/- 0.293 ppm, and Ni = 54.89 +/- 4.87 ppm. In contrast, the semi-rural reference station S6 recorded the lowest values: Pb = 24.91 +/- 3.27 ppm, Cd = 0.578 +/- 0.127 ppm, and Ni = 19.91 +/- 2.86 ppm. This contrast indicates a strong spatial contamination gradient and agrees with international evidence showing higher dust-bound metal concentrations around industrial margins, freight routes, mechanical workshops, high-traffic roads, and dense commercial areas [2-7].

The second-highest station was S3, the pilgrimage/religious district, with mean concentrations of Pb = 49.95 ppm, Cd = 1.791 ppm, and Ni = 46.72 ppm. This finding is locally important because Najaf has episodic increases in population density, traffic congestion, pedestrian movement, and commercial activity during visitation periods. These conditions can plausibly enhance road-dust re-suspension, vehicle emissions, brake and tyre wear, queueing, and short-term exposure among pedestrians and workers. Nevertheless, the present dataset cannot prove an independent pilgrimage effect because it does not include traffic counts, visitor-period indicators, exact sampling dates, or meteorological adjustment. The result should therefore be presented as a monitoring priority, not as causal attribution.

The temporal pattern was less influential than the spatial pattern. Mean concentrations declined from October to January and then increased again toward March, which is compatible with seasonal changes in dust activity and winter suppression of re-suspension. Similar regional studies have reported that dust storms and synoptic transport can affect particulate matter and dust chemistry in Iraq and surrounding areas [11-15]. However, in the current station-month matrix, month-level p-values were not significant for Pb, Cd, or Ni, so the discussion should avoid overstating seasonality or dust-storm causation without meteorological and event-specific evidence.

The statistical results strengthen the land-use interpretation. Station effects were significant for all three metals (ANOVA and Kruskal-Wallis $p < 0.001$), with high station eta-squared values (0.886-0.896), whereas month effects were not significant ($p = 0.597$-0.657). This means that the spatial difference among monitoring stations explained a much larger share of the observed variation than month-to-month fluctuation. The near-perfect inter-metal correlations ($r = 0.994$-0.999) further suggest co-located sources, simultaneous deposition, or a common dust-mass control rather than isolated metal-specific processes.

Health-risk assessment remains the main methodological limitation. Several road-dust studies calculate HQ, HI, and ILCR from dust-metal concentrations, but such calculations require validated pathway-specific exposure assumptions, toxicity values, and age-specific exposure parameters [3,7-10]. In the present dataset, AAS-based analytical determination and batch-level QA/QC are available, which strengthens the credibility of the measured metal concentrations. However, ppm dust values cannot be converted into inhalation exposure without air-volume or dust-loading metadata. Similarly, ingestion and dermal pathways require contact assumptions, ingestion rates, adherence factors, body weight, exposure duration, and toxicity-reference values. Reporting numerical HQ, HI, or ILCR values without these exposure inputs would create a false impression of precision. The defensible approach is to report hotspot prioritization now and reserve quantitative risk modelling for a follow-up dataset with complete exposure metadata.

5. Conclusions

The reconstructed station-month data identified a clear land-use-related spatial gradient in Pb, Cd, and Ni across Najaf. The dominant hotspots were the industrial-transport station S5, followed by the pilgrimage/religious station S3 and the high-traffic station S2, whereas the semi-rural reference station S6 consistently recorded the lowest concentrations. The statistical analysis confirms that spatial distribution and land-use type were the primary determinants of metal variation, while month-to-month variation was weaker and not statistically significant in the reconstructed matrix. Strong positive correlations among Pb, Cd, and Ni indicate a shared or co-located source profile or simultaneous deposition in the same dust mass. The AAS method and QA/QC procedures support the analytical reliability of the reported concentrations; however, definitive HQ, HI, and ILCR values should not be reported until exposure pathways, air-volume or dust-loading conversions for inhalation, toxicity-value selection, and age-specific exposure assumptions are fully verified.

6. Implications of policy and monitoring.

- Priorities: Confirmatory monitoring of S5 and S3 at normal and high-traffic conditions.
- Introduce meteorological logging indicators, dust-event classification and indicators of traffic/pilgrimage intensity to differentiate natural dust transportation and local anthropogenic sources.
- Report metal concentrations using unambiguous units and sample matrix: mg/kg dust, micrograms/filter, or micrograms/m 3 air.

Report metal-specific QA/QC values in the final journal article or supplementary file: reagent blanks, calibration blanks, calibration verification, spike recoveries, laboratory control samples, and LOD/LOQ for each investigated metal.

- HQ, HI, and ILCR are not used unless there are pathway-specific exposure assumptions which are tabulated and sensitivity analysis is performed on children and adults.

7. Limitations

This study is limited by the structure of the supplied files. The available results included station-month metal values, summary correlations, reported LSD values, and a general AAS/QA/QC description, but did not include a clean raw spreadsheet, verified coordinates, exact sampling dates, replicate-level laboratory measurements, metal-specific LOD/LOQ tables, air-volume measurements, dust-loading data, background concentrations for pollution-index normalization, or defensible exposure parameters. Therefore, the statistical patterns can be reproduced at the station-month level, but final numerical health-risk estimates cannot be defended from the current dataset alone.

Ethics statement

Not applicable. The study uses environmental monitoring data and does not involve human participants or biological specimens.

References

[1] Al-Dulaimi, E. M., Shartooh, S. M., & Al-Heety, E. A. (2021). Concentration, distribution, and potential sources of heavy metals in households dust in Al-Fallujah, Iraq. Iraqi Geological Journal, 54(2F), 123-136. https://doi.org/10.46717/igj.54.2F.11ms-2021-12-28

[2] Zglobicki, W., & Telecka, M. (2021). Heavy metals in urban street dust: Health risk assessment (Lublin City, E Poland). Applied Sciences, 11(9), 4092. https://doi.org/10.3390/app11094092

[3] Alghamdi, A. G., EL-Saeid, M. H., Alzahrani, A. J., & Ibrahim, H. M. (2022). Heavy metal pollution and associated health risk assessment of urban dust in Riyadh, Saudi Arabia. PLOS ONE, 17(1), e0261957. https://doi.org/10.1371/journal.pone.0261957

[4] Huang, C., Zhang, L., Meng, J., Yu, Y., Qi, J., Shen, P., Li, X., Ding, P., Chen, M., & Hu, G. (2022). Characteristics, source apportionment and health risk assessment of heavy metals in urban road dust of the Pearl River Delta, South China. Ecotoxicology and Environmental Safety, 236, 113490. https://doi.org/10.1016/j.ecoenv.2022.113490

[5] Shahab, A., Hui, Z., Rad, S., Xiao, H., Siddique, J., Huang, L., Ullah, H., Rashid, A., Taha, M., & Zada, N. (2022). A comprehensive review on pollution status and associated health risk assessment of human exposure to selected heavy metals in road dust across different cities of the world. Environmental Geochemistry and Health. https://doi.org/10.1007/s10653-022-01255-3

[6] Gupta, V., Bisht, L., Arya, A. K., Singh, A. P., & Gautam, S. (2022). Spatially resolved distribution, sources, exposure levels, and health risks of heavy metals in <63 micrometer size-fractionated road dust from Lucknow City, North India. International Journal of Environmental Research and Public Health, 19(19), 12898. https://doi.org/10.3390/ijerph191912898

[7] Mahmoud, N., Al-Shahwani, D., Al-Thani, H., & Isaifan, R. J. (2023). Risk assessment of the impact of heavy metals in urban traffic dust on human health. Atmosphere, 14(6), 1049. https://doi.org/10.3390/atmos14061049

[8] Jeong, H., & Ra, K. (2022). Pollution and health risk assessments of potentially toxic elements in the fine-grained particles (10-63 micrometer and <10 micrometer) in road dust from Apia City, Samoa. Toxics, 10(11), 683. https://doi.org/10.3390/toxics10110683

[9] Faisal, M., Wu, Z., Wang, H., Hussain, Z., Zhou, Y., & Wang, H. (2022). Ecological and health risk assessment of dissolved heavy metals in the urban road dust. Environmental Pollutants and Bioavailability, 34(1), 102-111. https://doi.org/10.1080/26395940.2022.2052356

[10] Taye, A. E., & Chandravanshi, B. S. (2023). Health and ecological risk assessment of potentially toxic metals in road dust at Lalibela and Sekota towns, Ethiopia. Environmental Monitoring and Assessment, 195, 765. https://doi.org/10.1007/s10661-023-11406-3

[11] Hilal, R. R., & Manii, J. K. (2024). Dust storm effects on air quality and particulate matter pollution in Babylon Governorate, Iraq. Iraqi Geological Journal, 57(1D), 17. https://doi.org/10.46717/igj.57.1D.17ms-2024-4-27

[12] Hamed, A. M., & Al-khakani, E. (2024). Synoptic conditions at pressure different levels for the dust storm of May 2022 over Iraq. Indonesian Journal of Geography. https://doi.org/10.22146/ijg.93329

[13] Ismail, R. R., Al-Abudi, B. Q., & Halos, S. H. (2024). Spatial and temporal analysis of severe dust storm in Iraq in May 2022. Iraqi Journal of Science, 65(10 SI), 5933-5947. https://doi.org/10.24996/ijs.2024.65.10(SI).4

[14] Mohammed, M. I., Abid, M. F., Albassam, I., Abdullah, H. M., Abdul Razak, A. A., Mahmoud, M. A., Alaq, E. K., & Aswed, F. M. (2024). Characterization of minerals and health impact of metals in dust storm fallen on Baghdad, Iraq. Asian Journal of Water, Environment and Pollution, 21(1). https://doi.org/10.3233/AJW240008

[15] Al Nadhairi, R., Al Kalbani, M., Al Khazami, S., Al Hashmi, M., Al Zadai, S., Al-Rumhi, Y., & Al-Kindi, K. M. (2025). Air quality and health risk assessment during Middle Eastern dust storms: A study of particulate matter. Air Quality,

Atmosphere & Health, 18, 587-603. https://doi.org/10.1007/s11869-024-01662-8

[16] MacFarland, T. W., & Yates, J. M. (2016). Kruskal-Wallis H-Test for Oneway Analysis of Variance (ANOVA) by Ranks. In Introduction to Nonparametric Statistics for the Biological Sciences Using R (pp. 177-211). Springer. https://doi.org/10.1007/978-3-319-30634-6_6